UC San Diego

UC San Diego Electronic Theses and Dissertations

Title

Contribution of CA3 sharp-wave ripple oscillations to decision making during complex spatial working memory tasks

Permalink

https://escholarship.org/uc/item/9n62b6xg

Author

Vartanian, Adeh

Publication Date

2021

Peer reviewed|Thesis/dissertation

eScholarship.org Powered by the California Digital Library
University of California

UNIVERSITY OF CALIFORNIA SAN DIEGO

Contribution of CA3 sharp-wave ripple oscillations to decision making during complex spatial working memory tasks

A Thesis submitted in partial satisfaction of the requirements

for the degree Master of Science

in

Biology

by

Adeh Vartanian

Committee in charge:

Professor Jill Leutgeb, Chair
Professor Ashley Juavinett
Professor Stefan Leutgeb

2021

©
Adeh Vartanian, 2021
All rights reserved.

The thesis of Adeh Vartanian is approved, and it is acceptable in quality and form for publication on microfilm and electronically.

University of California San Diego

2021

DEDICATION

To my parents, I can't thank you enough for all that you have given me. I would have never been in the position I am today if it wasn't for your countless sacrifices. I am forever grateful for your love and support. This thesis is for you!

TABLE OF CONTENTS

LIST OF ABBREVIATIONS

MTL Medial Temporal Lobe

DG Dentate Gyrus

PHR Parahippocampal Region

EC Entorhinal Cortex

mEC Medial Entorhinal Cortex

lEC Lateral Entorhinal Cortex

WM Working Memory

LFP Local Field Potential

SWR Sharp-Wave Ripple

SW Sharp Wave

LMF Low Mossy Fiber

vHC Ventral Hippocampal Commissure

PFA 4% Paraformaldehyde

PBS Phosphate Buffered Saline

EMA Exponential Moving Average

LIST OF FIGURES

ACKNOWLEDGMENTS

I would like to express my sincerest gratitude for Dr. Jill Leutgeb. As the principal investigator of my project, her mentorship has been invaluable in my growth as a scientist. She has taught me a way of thinking that will advance my career not only in research, but also in all facets of life. Thank you for your continued guidance and support in my journey.

I would also like to recognize Dr. Stefan Leutgeb for his assistance and support in my project. I greatly appreciate your help and advice throughout this process.

I would also like to recognize Dr. Ashley Juavinett for serving as a committee member and an advisor to all master's students in the department. Thank you for all your efforts.

I look up to every individual on my committee and model my professionalism and attitude after them as they have set perfect examples in every regard. I am thankful to have learned from your indispensable experiences and hope to one day pass this knowledge on to future generations.

I would also like to thank Yudi Hu and Ameen Khan for all their support and friendship as we navigated this journey together as well as Li Yuan for always being there for advice.

Finally, I would like to thank each and every individual in the Leutgeb Labs for always lending a helping hand. This project would not have been possible without you all.

VITA

2020	Bachelor of Science, University of California San Diego
2020	Teaching Assistant, Department of Biological Sciences, University of California San Diego
2020-2021	Graduate and Professional Student Association Representative, Department of Biological Sciences, University of California San Diego
2021	Teaching Assistant, Department of Psychology, University of California San Diego
2021	Master of Science, University of California San Diego

FIELD OF STUDY

Major Field: Biology

Studies in Neurobiology and Neurophysiology
Professor Jill Leutgeb

ABSTRACT OF THE THESIS

Contribution of CA3 sharp-wave ripple oscillations to decision making during complex spatial working memory tasks

by

Adeh Vartanian

University of California San Diego, 2021

Professor Jill Leutgeb, Chair

Many regions of the brain contribute to memory processing and the subsequent use of stored memories for making informed decisions. The hippocampus is a known region in the medial temporal lobe that can support spatial working memory through interconnections between its distinct sub-regions when the information being held is complex. The synaptic connections in play include the mossy fiber pathway which carries information from the dentate gyrus (DG) to the CA3 recurrent cell layer. Studies have demonstrated that DG lesions effectively impair spatial working memory during complex memory tasks. Local field potential studies have observed the onset of 150-250Hz oscillations, characterized as sharp-wave ripples (SWR), in the

CA3 cell layer during working memory. These fast oscillations were correlated with subsequent correct choices and were also found to be DG dependent. Therefore, we hypothesized that working memory is supported by SWR oscillations generated by DG inputs to the CA3 cell layer. Our project aimed to test this casual role through the inhibition of CA3 SWR oscillations in rats during a dentate-dependent working memory task on an 8-arm radial maze. We implemented a SWR detection program to accurately detect high frequency events in CA3 known to be SWRs. Upon detection, electrical stimulation of the ventral hippocampal commissure was triggered, inhibiting SWR generation in CA3 through the prolonged silencing of hippocampal neurons. Behavioral performance was then quantified for stimulation trials and compared to no-stimulation control trials. We observed no significant impairment in memory performance when SWR oscillations were inhibited compared to control trials. This finding suggests the generation of CA3 SWRs does not play a casual role in spatial working memory and is not essential for ongoing decision-making during such tasks, but the conclusion remains to be tested in a larger cohort of animals.

INTRODUCTION

As one of the primary functions of the brain, memory processing takes place every day to complete anything from mundane tasks to critical analysis of complex problems. Memory is classically defined as the process by which what is experienced or learned persists across time (Ebbinghaus, 1880). Memory is appropriately classified into different types which carry out different functions and are supported by different brain regions. Without the proper processing of these memory functions, even the simplest tasks may become impossible, and life unsustainable. Therefore, further defining and understanding the mechanisms underlying different types of memory will facilitate the development of new treatments for patients suffering from amnesia and other memory disorders such as Alzheimer's disease.

Where is Memory Stored?

During memory formation, the brain encodes pieces of information and stores those it finds useful to be accessed at a later time (Müller and Pilzecker, 1900). In 1950, Karl Lashley proposed the Law of Mass Action which declared that memories are not stored in a single center in the brain (Lashley, 1950). He instead suggested memories are intertwined between several regions of the brain as he noted that the extent of damage to the brain, not the specific location of the damage, is what determines the deficit in memory (Lashley, 1950). The site of memory storage, or the so called "engram", is a widely-explored concept which has so far identified candidate regions as physical storage locations in the brain. In 1938, Wilder Penfield proposed that aspects of memory may be stored in the medial temporal lobe (MTL) of the brain (Penfield, 1938). In a clinical study, Penfield selectively removed epileptic tissue in patients suffering from

seizures to relieve symptoms. He then stimulated the MTL where he witnessed the patients encounter coherent experiences (Penfield & Boldrey, 1938).

Different Regions Control Different Aspects of Memory

Many similar studies followed, including that of patient H.M. which further established the MTL as the central hub of memory. In his case, patient H.M. underwent a bilateral temporal resection as treatment for his debilitating seizures (Scoville & Milner, 1957). The bilateral lobectomy left H.M with anterograde amnesia, which is the inability of forming new memories, while still retaining old childhood memories (Penfield & Milner, 1958). Moreover, H.M.'s motor memory also remained intact suggesting that distinct types of memory are supported by different regions of the brain (Scoville & Milner, 1957). One important region in the MTL is the hippocampus which proved to play a role in declarative memories (Penfield & Milner, 1958). The two overarching types of memory are short-term and long-term memory, which encompass all other forms of memory (Reber et al, 1998). Short-term memory consists of immediate and working memories while long-term memory consists of two subcategories, implicit and explicit (Reber et al, 1998). Explicit, or declarative, memory is conscious memory which includes episodic and semantic memories such as events and common world news. On the other hand, implicit, or non-declarative memory is unconscious and includes procedural memory such as motor-functions like driving (Reber et al, 1998).

As a distinct region in the medial temporal lobe, the hippocampus serves in processing and retrieving spatial memories essential for spatial navigation (Morris et al, 1982). This was demonstrated in a task where rodents were placed in an opaque pool in a room with several spatial cues. The rodents were then trained to locate an escape platform placed underwater in order to exit the pool. The pool was also assigned quadrants with the escape platform in one of

the quadrants to help track the performance of the rodents in the task based on time spent in a specific quadrant. The study showed rodents with hippocampal lesions spent significantly more time searching in incorrect quadrants rather than control groups who spent most of their time in the target quadrant (Morris et al, 1982).

Hippocampal Anatomy

In better understanding the hippocampus, its structure and connectivity provide insight on the functionality of the region and how memory is processed. As an extension of the cerebral cortex, the hippocampus is a curved, S-shaped structure with densely populated layers of neurons laying on the border of the temporal lobe (Anand et al, 2012). The hippocampus is primarily comprised of two parts which ultimately carry out its functions, the hippocampus proper and dentate gyrus (DG) (Anand et al, 2012). The hippocampus proper contains the CA1 and CA3 cell layers which are connected to one another through a defined pathway, known as the schaffer collateral pathway, projecting information from the CA3 up to the CA1 cell layer (Green, 1964). The hippocampus proper communicates with the DG through the mossy fiber pathway which is the series of axons that connect dentate granule cells to CA3 cells (Green, 1964). Lastly, the perforant pathway serves as the connection between the entorhinal cortex and the DG. In addition to these intrahippocampal connections, the different layers also receive inputs from the surrounding parahippocampal region (PHR) which includes the entorhinal cortex (EC), perirhinal cortex, postrhinal cortex, presubiculum and parasubiculum (Strien et al, 2009). The EC, subdivided into the medial entorhinal cortex (mEC) and lateral entorhinal cortex (lEC), is in direct connection with all hippocampal layers. These networks propagate signals received from the PHR and signal to the different parts of the CA1, CA3, and DG regions through both the

mEC and lEC (Strien et al, 2009). It is through these intertwined networks that the hippocampus is able to perform its role in memory processing.

Role of Dentate Gyrus and CA3 in Hippocampus

As a sub-region in the hippocampal formation, the DG plays an essential role in complex working memory (WM) tasks as DG lesions effectively impair behavioral performance during such tasks (Xavier et al, 2009). This was observed in studies where the DG in rodents was injected with colchicine, a neurotoxin, to selectively remove dentate granule cells and performance was measured during WM behaviors (Xavier et al, 2009). The resulting deficits were credited to the specialized firing patterns in DG that are conveyed to CA3 through the projections from the DG (Xavier et al, 2009). The CA3 is an auto-associative network meaning it contains recurrent synaptic connections (Treves & Rolls, 1991). These recurrent connections allow the CA3 region to process pattern completion with excitatory synapses projecting back onto CA3 cells in the same layer (Treves & Rolls, 1998). This enables the retrieval of ensembles which can be reactivated after a partial cue activates a subset of the cells in the network ensemble. Synaptic plasticity of these cells also allows these ensembles to form or disassemble as needed in forming new memories or discarding old ones (Nakazawa et al, 2002; Nabavi et al 2014). This is essential for memory consolidation and retaining complex spatial WM while the role of the DG through its projections is to initiate pattern separation which is critical for memory retrieval (Treves & Rolls, 1991).

Pattern separation is the mechanism that supports encoding memories distinctly from one another to help differentiation between them during retrieval. Processing of pattern separation in the DG was confirmed with the analysis of dentate granule cells and cells recruited in the CA3

when rats explored two different environments. It was shown that inputs from the DG activated new CA3 ensembles when the environment presented to the animal changed (Leutgeb, 2007). Further studies proved this mechanism to be present in the human hippocampus as fMRI displayed pattern separation-biased activity in the CA3 and DG unlike pattern completion-biased activity in CA1 and PHR (Bakker et al, 2008). These highlighted functions reveal the importance and necessity of hippocampal subregions in performing different functions in support of memory.

Place-cells and Place-fields

All hippocampal subsections also contain specialized cells, termed place-cells, that code for coordinates and environmental cues to help the organism identify its relative position at any given moment (O'Keefe et al, 1971). These cells have been observed to preferentially fire at specific locations in space which ultimately gives the host geographic data and a sense of location (O'Keefe et al, 1971). Each place-cell possesses a so called "place-field" where the cell will fire if the host enters that area. Besides providing geographic information, place-cells also exhibit differential firing during ongoing behavioral tasks (Wood et al, 2000). This was observed in a spatial alternation task on a T-maze where certain place-cells on the common path between left and right trials were activated only during either left or right turn trials (Wood et al, 2000). It has been demonstrated that the firing rates of place-cells change when features around a given location change, relaying detailed information, such as color or shape, regarding the surroundings to the host (Leutgeb et al, 2005). This falls in line with the idea that hippocampal neurons not only possess a place code, but also a rate code, distinguishing various environments from one another (Leutgeb et al, 2005).

Hippocampal Oscillations

In addition to a place code and a rate code, spike timing can also convey meaningful information to the host. Brain oscillations have been observed to organize spike timing. To better understand the underlying process, brain oscillatory activity can be observed and analyzed via local field potential (LFP) recordings. LFP studies allow for the classification and interpretation of set oscillatory activities through visualization and in-depth analysis of such waves. This approach provides insight on the mechanism of the temporal firing coordinated by distinct oscillatory activity. Characterized oscillations seen in the hippocampus include theta, gamma, and sharp-wave ripple (SWR) oscillations which play their respective roles in various memory functions (Bragin et al, 1995; Colgin, 2016). Each oscillation is unique in its frequency, which is how they are ultimately defined and labeled. Studies have shown theta oscillations (7-9 Hz) to be present when the subject is in an exploring phase, moving around, and absent during periods of immobility except REM sleep (Vanderwolf, 1969). Gamma oscillations (30–90 Hz) can be seen throughout different states, but are typically observed during alert states such as when a subject is encoding or retrieving memories (Csicsvari et al, 2003). Contrary to theta oscillations, SWRs are characterized as hippocampal oscillations in the 150-250Hz range which are primarily seen during stationary resting states as well as in slow-wave sleep (Frank & Joo, 2018). SWRs may be detected in the CA3 and CA1 regions of the hippocampus (Buzsáki, 1986). The different oscillatory frequencies listed appropriately time hippocampal networks and underlie different network computations essential for various memory functions.

SWR Generation

To better understand SWRs and their role in memory, research has been conducted on not only where, but how they are generated. Several manipulation studies have confirmed the origination of sharp-wave (SW) oscillations from the hippocampal region. In these studies, the hippocampus was isolated with the lesion of surrounding regions such as the entorhinal cortex (Suzuki and Smith, 1988). This allowed for the focused inspection of oscillatory activity from the hippocampus only, which revealed the permanence of SW events even in the absence of surrounding regions (Jouvet et al, 1959; Buzsaki et al, 1983; Ylinen et al, 1995). Furthermore, the recurrent circuit present in the CA3 layer is known to generate population bursts through its recurrent excitations (Wittner et al., 2007). This initiation of population bursts is the default activity of recurrent networks and the inhibition of suppressive neuromodulators at reward consumption and slow-wave sleep give rise to synchronized neuronal bursts identified as SWRs in LFP recordings (Buzsaki et al, 1983). This activity is then propagated through schaffer collateral axons up to the CA1 layer as seen in current source density maps displaying the depolarization of CA1 neurons in response to CA3 discharges (Sullivan et al, 2011).

Content of SWR

The information transmitted by the subset of neurons selectively activated during ripple oscillations has piqued the interest of the field. Researchers have reasoned that the temporal activation of these neurons supports spatial memory through the replay of past experiences (Wilson & McNaughton, 1994). Replay refers to the phenomenon that groups of neurons activated together during awake behavior are seen to collectively fire again in sleep sessions (Wilson & McNaughton, 1994). Based on the place cells that are activated in behavior, it was

observed that replay of place cell sequences can code for forward and reverse paths (Wilson & McNaughton, 1994). Other studies have also shown that SWRs detected during sleep stages contribute to memory consolidation. Accordingly, the disruption of SWRs during sleep results in impairment on a spatial memory task (Girardeau, et al 2009). Moreover, disruption of CA1 SWR events in rats has shown to also impair the learning of working memory tasks as subjects took longer to learn the task when SWRs were disrupted (Jadhav et al, 2012). Furthermore, it is hypothesized that SWRs during stationary rest periods at reward points retrieve information of experiences from the immediate past and apply it in future decision making (Frank & Joo, 2018). This interpretation implies that the content of replay only includes experiences involved in the ongoing behavioral trial. However, this explanation is not consistent with deeper analysis of replay content, which shows that reactivated place fields were more representative of the overall environment rather than specific experienced pathways (Gupta et al, 2010). The conclusion that a more general cognitive map is represented is based on the observation that never-experienced "shortcut" sequences are replayed at reward locations in the maze (Gupta et al, 2010). These sequences were therefore not only replaying the animals' immediate past location, but rather represented paths the animal had not even traversed before. Better yet, these "shortcut" sequences were viable routes the animal could take to reach a reward site (Gupta et al, 2010). These findings imply that the content of SWR may be useful for decision making as it provides information about the past and informs future actions.

Contribution of Place-cells in Ripple Activity

Expanding on how spatial trajectories are assembled, further studies have demonstrated how hippocampal place cells code for future routes that an animal is planning to take (Foster and

Pfeiffer, 2014). This was shown in an open maze task with 36 different wells, where one well was assigned to be the *home* location and other wells were *random* reward locations that were changed for each new trial. Hippocampal neurons were recorded from the CA1 region and their place fields were identified through analyses of firing patterns. In addition to standard place fields, the recordings also revealed that compressed firing of place cells coincides with SWR activity during periods of immobility in the task. Moreover, these compressed events corresponded to trajectories toward known goal locations such as *home* when the animal was at a *random* location thereby over-representing the current *home* location. To confirm the trajectories reflected navigational guidance to the animal's next desired location, the angular displacement between the trajectory and the actual path to the goal location were calculated. The data displayed negligible angular difference between the pre-played future trajectories and the path taken by the animal (Foster and Pfeiffer, 2014). The representation of the past path, however, was not matched, which suggests that the computed trajectories coded for future paths rather than past locations. Therefore, given the utility of place cells, they are hypothesized to be essential for spatial working memory tasks and their firing during SWR oscillations suggests a correlation between the two in the decision-making process of such tasks (O'Keefe et al, 1971). Nonetheless, the role carried out by SWR events and whether they directly contribute to active WM functions is unknown.

CA3 SWR

While CA1 SWRs have been extensively analyzed, much less is known about the potential role of CA3 SWRs in memory. As mentioned previously, both hippocampal SWR and DG activity are necessary in complex spatial working memory tasks (Jadhav et al, 2012; Xavier

et al, 2009), but a connection would have to be mediated by CA3 given that DG projections selectively terminate in the CA3, but not the CA1 sub-region. Intrigued by a potential connection between the necessity of the DG and SWRs for memory, Sasaki et al. (2018) set out to identify a mechanistic correlation between the regions which ultimately enables functioning working memory in rats. To test this hypothesis, rats were trained to perform a spatial working memory task on an 8-arm radial maze while recordings of neuronal activity from hippocampal cell layers were obtained. Analysis of neuronal firing patterns revealed close temporal pairing of DG neuronal firing and SWR incidence which were most prominent at reward sites on the maze (Sasaki et al, 2018). Analysis revealed that DG cells preferentially fired ~1 second after reward consumption and that CA3 SWR rates increased immediately thereafter (Sasaki et al, 2018). Furthermore, analysis of place cells that were reactivated during SWR oscillations suggested a difference in the content of SWRs in DG lesioned vs control animals. Rats with DG lesions that had either no or low mossy fiber (LMF) input to CA3 were compared to rats with an intact DG. The firing of identified CA3 place cells revealed far more prospective firing of place cells in control animals in comparison to LMF animals where the ratio of prospective and retrospective firing was more similar (Sasaki et al, 2018). Prospective firing refers to the firing of place cells on arms that were not yet visited and that the animal had to visit to complete the task. This is a potential mechanism to explain why animals with an intact mossy fiber pathway performed significantly better on the task than LMF animals. It was also observed that the incidence rate of SWRs during the reward period increased in control animals but not in LMF animals (Sasaki et al, 2018). This leads to the conclusion that DG inputs to the CA3 result in an increase in neuronal firing rates and SWR activity at the reward sites.

Taken together, these findings suggest that DG input to the CA3 support CA3 SWRs and that CA3 SWR oscillations may be necessary for performing complex spatial working memory tasks. This study is first to propose that the DG does not only support pattern separation, but also supports working memory by facilitating SWRs in the CA3 layer of the hippocampus. The study also established a positive correlation between the incidence rate of SWR events and correct decision making during the memory task. This raises the question whether CA3 initiated SWRs aid in the decision-making process and directly contribute to correct choices during working memory behavior.

Goal of Project

Given that the necessity of CA3 SWRs for ongoing decision-making in a dentate-dependent working memory tasks has not been established, my project aims to test the causal role of CA3 SWRs for supporting of working memory. Previous findings – the replay of future sequences during SWR events and their correlation with correct decision making on memory tasks - have supported the idea that spatial memory performance is supported by SWRs (Foster and Pfeiffer, 2014; Sasaki et al, 2018). Thus, we predict that CA3 SWRs code for future choices by allowing for the firing of CA3 cells with place-fields on not-yet-visited arms of the maze. Previous studies addressing SWRs lacked two aspects which my project will be addressing. First previous studies used linear or two-choice mazes, which increases the likelihood of correct decisions due to chance and lacks complexity. In my project, an 8-arm radial maze will be utilized, where the animals will have 8 options to select from when making a decision. This reduces the likelihood of correct choices due to chance and provides much greater statistical power in measuring performance accuracy. Therefore, this task will be much better suited for the

purposes of my project and addressing the question at hand. Another point that is not addressed in previous studies is whether it is the decision about the next choice or the slow improvement in performance that is dependent on SWRs. In previous studies, CA1 SWRs were inhibited during the acquisition phase of memory. Instead, my project will be inhibiting CA3 SWRs after asymptote performance has reached to test whether there are any immediate effects on memory retention in a working memory task. The experiments will be performed by recording hippocampal LFP signals and single-units in freely behaving rats. SWR events during behavior will be detected, and brain stimulation will be delivered that silences hippocampal CA3 cells immediately after the onset of a SWR event. Memory performance will then be measured and analyzed to reveal whether SWR disruption results in memory deficits. Using these methods, we will be able to test the causal role of SWRs in supporting ongoing decision making during working memory.

CHAPTER I – METHODS

Approvals

All implemented methods were approved by the Institutional Animal Care and Use Committee at the University of California, San Diego and corresponded to National Health Institutes guidelines

Subjects

For this study, 8 male Long Evans rats, weighing between 350g-375g were trained and implanted with a chronic recording array. Behavioral recordings were obtained from 7 of these animals and only 4 were included in the final analysis of data. One animal was implanted but never recorded from due to health complications. Based on set criteria, animals were deemed either qualified or unqualified to be included in the study. Animals were rejected if the implanted drives produced uncontrolled noise disrupting the spike sorting of cells and successful analysis of LFP data (N = 2 rats). Animals were also rejected if they displayed epileptic characteristics post-surgery or experienced any form of unintentional seizures due to stimulation during experiments (N = 1 rat). Subjects included in the study performed the behavioral task at the set criterion of 80% correct, were implanted successfully with no complications, and presented reliable and sufficient data for collection (4 out of 7 trained rats). A total of 4 additional animals were utilized in the methods development process for this study. Each animal was housed in its individual home cage in a vivarium setting on a reverse light schedule. Subjects were placed under food restriction after arrival in the vivarium and were maintained at 85% of their starting weight while continuing with an unlimited water supply.

Behavioral Task

All subjects in this study were trained on an 8-arm radial maze which is known to be a complex, dentate-dependent spatial working memory task (Sasaki et al, 2018). The maze is made of black Plexiglas with a stationary octagonal center stem where the animals begin the task. Eight individual arms, made of the same Plexiglas material, extend 79 cm from the center stem in each direction (Figure 1). Each arm is raised or lowered semi-automatically through a remote switch to control access to each arm. The end of each arm contained a reward location wired with a sensor used for detecting precise time when each reward was consumed. The reward of choice was a chocolate powder and water solution (0.2 mL).

During the 12-hour dark period of the animal's day, behavioral testing was conducted in a dimly lit room, with certain constant spatial cues present including a small desk lamp that was kept on the west side of the maze. The task began when the animal was placed on the center stem with all the surrounding arms lowered, restricting movement off the stem. For the forced phase of the task, single arms were sequentially raised until the subject had entered 4 of the 8 arms. Upon consumption of reward on the 4^{th} arm, all 8 arms were raised simultaneously, marking the start of the choice phase. At this stage, the animal had the option to enter any arm on the maze, in search of the 4 remaining rewards. Once all rewards were found and consumed, all the arms were lowered and the animal returned to the center stem.

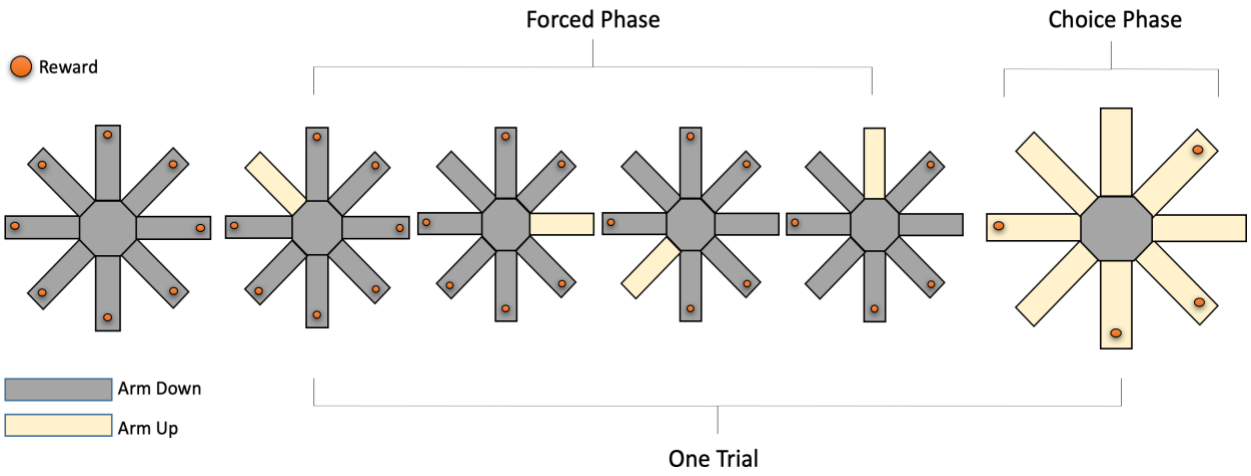

Figure 1. 8-Arm Radial Maze Spatial Memory Task. Rodents were trained to search and retrieve chocolate-drop rewards at the end of each arm. During the "Forced Phase", animals were sequentially guided down 4 pseudo-randomly selected arms, after which all arms were made available for the "Choice Phase". Animals were trained on this task until they reached a criterion of 80% correct trials.

Handling & Habituation

When ordered rats arrived from Charles River Laboratory at our facility, they were housed in their own cages. To accustom subjects to human interaction and touch, they were lightly handled for 2-3 days. During this time, the rats were handled in the home cage to feel safe and comfortable. Later, subjects were placed in a new environment and were handled there to establish a safe relationship with the trainer. Once subjects were comfortable being handled, they transitioned into a habituation period. During this period, rats were placed on the 8-arm radial maze in exact experimental conditions, except all arms were initially raised and the subjects were free to roam around the maze. This was done to familiarize the animals to the task and maze environment. At this stage, animals learned spatial cues present in the behavior room, became aware of the rewards present at the end of each arm, and felt safe moving around the maze with no hazard present.

Training

Training on the memory task typically began after 3 days of habituation when the subject was moving around the maze comfortably and was consuming all the rewards. At this point, rodents were subject to the "Forced" and "Choice" phases of behavior. For behavioral sessions, new pseudorandomized "Forced" sequences were generated for every trial, excluding sequences where the animal was set to enter 3 arms in sequential order (i.e. 4, 5, 6) to prevent an undesirable habit of entering arms in order, rather than searching. Once the animal had entered the four "Forced" arms, all arms were raised and the animal was required to search for the not-yet-visited arms in that trial. Reentry into already visited arms were noted as incorrect attempts. After consumption of all available rewards or a time limit of 10 minutes every arm was lowered, and the animal returned to the center stem. At this stage, one trial was completed, and the animal rested on the center stem for 2 minutes awaiting the next trial while rewards were re-baited on each arm. Rats were trained to perform 1 hour long sessions where they completed as many trials as possible in that time frame. Behavioral performance was calculated based on arms visited in search of the 4 remaining "correct" arms. Therefore, accuracy was determined as 4 attempts divided by number of total arms visited in each trial. Subjects were trained until they reached the set criterion of 80% performance accuracy during sessions prior to implantation. This was achieved within an average of 10±2 days across animals.

Subjects were retrained on the same exact task 5 days post-surgery, except with the addition of the implanted hyper-drive (see Surgery Section). The head-stage allowed for electrophysiological recordings through a connected lightweight multiwire tether. Training and turning took place concurrently until subjects reached the criterion of 80% accuracy again, with occasional days of recording for data collection. At the time of experimental recordings, subjects

performed at or above 80% accuracy and completed between 18-21 trials in hour long sessions with 2 “sleep” periods before and after the task (Figure 2).

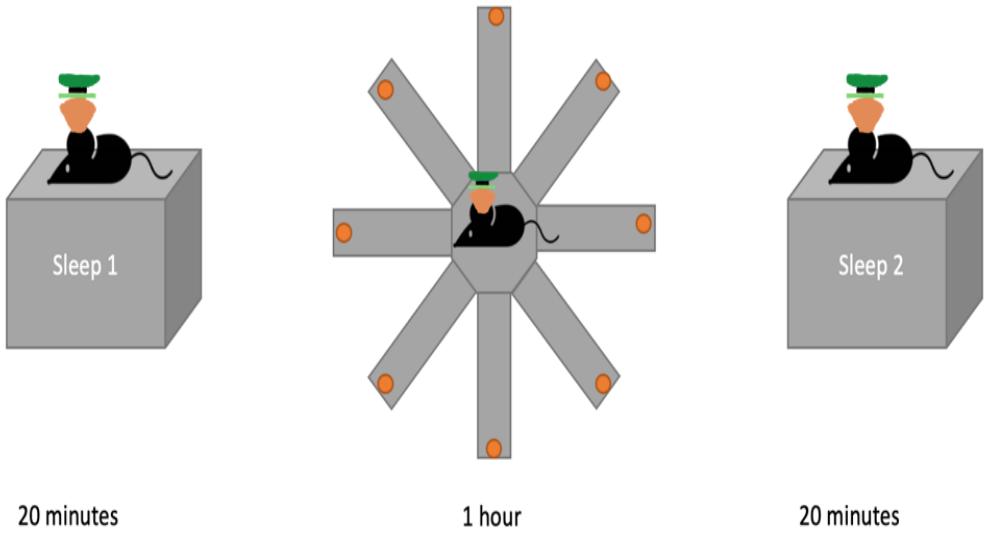

Figure 2. Working Memory Recording Paradigm. Each recording session included two “sleep” sessions, one preceding and one following the spatial memory task. For each “sleep” session, animals rested for 20 minutes in a familiar bin while recordings were obtained. Longer “sleep” sessions were warranted if the animal remained hyperactive and did not enter slow-wave sleep.

Surgery

The same surgical hyper-drive implantation took place in all 7 recorded animals. The tetrode bundle in each drive, comprised of 14 individually movable tetrodes, was carefully placed above the right dorsal hippocampus. Coordinates, 4 mm posterior and 3 mm lateral to bregma, were used to accurately estimate the target location in the hippocampus. Each tetrode was made of 4 twisted platinum wire electrodes (4-6 microns, California Fine Wire) that were plated with platinum to lower resistances to the desired range (see Mankin et al, 2015). Two bipolar stimulating wires were placed in the ventral hippocampal commissure (vHC), one in each hemisphere. They were gently lowered 3.6 mm deep in the region during surgery, where they remained for the duration of experimentation. In preparation for surgery, rats were anesthetized

with isoflurane gas (2-2.5 % in O_2) and Buprenorphine (0.05 mg/kg) was injected as the analgesic of choice. The hyper-drive was fixed onto the subject's head with stainless steel screws and secured with dental cement.

Tetrode Turning

The implanted hyper-drive is composed of a bundle of 14 tetrodes which can be moved independently along a screw thread. The bundle was placed above the right hippocampus, as described above (Surgery). The tetrodes that were immediately lowered 960 microns following surgery. In the following days post-surgery, electrodes were slowly turned down to target locations with the goal of recording action potentials from principal neurons as well as local field potentials. Local field potential (LFP) depth profiles were used to identify characteristic patterns such as theta and SWR oscillations, along with their polarities, to estimate tetrode location. Out of the 14 available tetrodes, two were assigned as reference tetrodes (Reference 1 and 2). Reference 1 was kept in the cortex as a differential reference while Reference 2 was lowered to the hippocampal fissure to obtain local hippocampal LFP. The other 12 tetrodes were periodically lowered down to the CA1 layer at first and eventually to the CA3 cell layer for recordings. Typically, 1 or 2 tetrodes remained in the CA1 cell layer to enable recording of CA1 cells and SWRs simultaneously with CA3. The turning process took approximately 9-10 days, with large advancements being made early on and turning in small increments when approaching cells. Tetrodes were allowed to settle into the cell layer prior to recording days to optimize stability of units. Tetrode locations were adjusted as needed prior to or after recordings, but no experiments were conducted within 4 hours of turning. Tetrode locations were identified using postmortem histology as described below (Tetrode Tracking).

Recording Apparatus

A digital Neuralynx recording system was used in the collection of electrophysiological data from hyper-drive implanted subjects. In this closed-loop apparatus, the Neuralynx system obtained in-vivo local field potential (LFP) and unit spiking from the positioned tetrodes and processed this information through the proprietary software (Cheetah, Neuralynx). This information was then communicated to other software including Xilinx and MATLAB which ultimately processed the detection logic for disrupting SWR oscillations. Moreover, an Arduino board interfaced with Xilinx and a Master 8 box to control the stimulation logic employed in each experiment. Xilinx processed a maximum of 4 selected ports from Cheetah, corresponding to 4 different manually assigned tetrodes. Upon detection of SWR events on the assigned ports, Arduino is informed by Xilinx and a decision to deliver a stimulus is rendered based on the coded logic. Stimulation was deployed from 2 IsoFlex devices controlled by the Master 8 which received input from the Arduino board. Integrating electrophysiological data from Cheetah and detection instructions from Xilinx and MATLAB, Arduino allowed for the triggering of stimulation upon detection. Various functions were selected by the experimenter, and implemented through Arduino, in different experiments including "AND" and "OR" functions. The "AND" function triggered stimulation upon the detection and coherence of SWR oscillations between all assigned ports. The "OR" function triggered stimulation upon the detection of SWRs on any of the assigned ports. Every detected SWR by Xilinx and stimulation onset by Arduino (TTL) was automatically marked in Cheetah with an associated timestamp. A schematic of the system is presented in Figure 3 below.

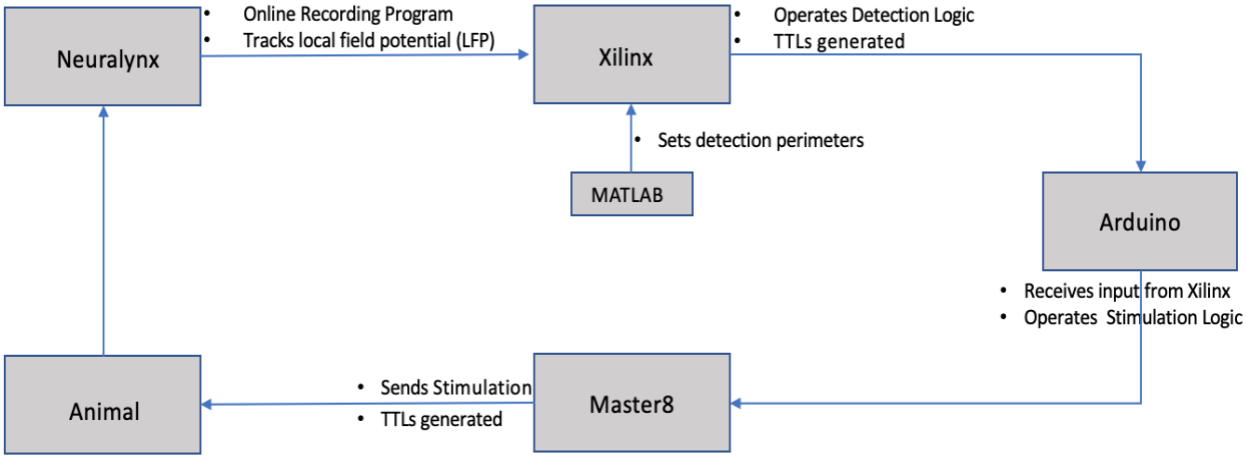

Figure 3. Closed-Loop Recording System. Schematic representation of the closed-loop recording system, with each module and its functions, enabling both the recording of hippocampal cells and stimulation of the vHC in each animal.

SWR Detection

Online detection was processed by the Xilinx software. During later offline data analysis, SWRs were also identified by calculating the root-mean-square power of 150 to 250 Hz bandpass-filtered LFP signals over 10ms intervals. A SWR event was defined as power exceeding 4 standard deviations from the mean amplitude (uV) on a given recording channel.

Disruption by Stimulation

Stimulating the ventral hippocampal commissure (vHC) elicits a large population burst in the hippocampal CA1 and CA3 layers, which results in a large and broad inhibition of the network following the input. The outcome of this network inhibition is the blocking of the remainder of the SWR. To achieve this effect, similar procedures to those reported in Jadhav et al, (2012) were implemented. Two bipolar stimulating wires were bilaterally placed in the vHC during surgery to enable stimulation of commissural fibers propagating within the hippocampal

region. Stimulation was conducted through one of the two assigned wires, which was selected prior to experimentation based on artifact characteristics.

Establishing Stimulation Perimeters

A series of stimuli of different strength were administered and the activity of hippocampal neurons in response to each stimulus assessed. Stimulation strength was determined prior to experimentation through the generation of spike-time histograms which display degree of inhibition in the hippocampal network for a given stimulation current (in pA). Level of inhibition is assessed for each stimulus strength by effectively generating a peristimulus time histogram of the spiking of a defined cell with respect to the stimulus artifacts and by defining the length (ms) of inhibition before the cell fires again (Figure 6A). An optimal inhibition period of ~100 ms was established in line with similar studies reported in the literature (Jadhav et al, 2012). The stimulus strength that best provided this range of inhibition with the lowest stimulation amplitude possible was selected to be used in future experiments with SWR detection. The stimulation strengths used in experiments and the inhibition periods achieved varied across animals, ranging from 100-180 pA in amplitude and 50-100 ms of inhibition, respectively. A lock-out period of 200 ms was included in-between each stimulation to limit the frequency at which stimuli were delivered and to avoid inducing undesired seizures.

Behavioral Experiments with Closed-Loop Stimulation

Once animals have reached the 80% performance accuracy criterion and viable cells are available for recording, the main experiment commenced. A day prior to experimental recordings, stimulation wires were tested and an I/O curve was established. In the following

days, several experiments were conducted as described below. Only one experiment type was completed per day as long as tetrodes remained in the target location with at least 5 clearly isolated cells to confirm inhibition levels for each experiment.

Stimulation upon SWR Detection

In this experimental setup, the online SWR detection program was utilized to stimulate the vHC and effectively inhibit the remainder of the SWR oscillations after detection in hippocampal CA1 and CA3 layers. Different stimulation logics were implemented through Arduino to either stimulate upon the detection of CA3 SWRs only or both CA1 and CA3 SWRs. With the availability of LFP from both CA1 and CA3 layers, "AND" or "OR" functions were executed to achieve inhibition of SWRs recorded from both regions. "AND" functions enabled the inhibition of SWRs when there was coherence in ripple activity between CA3 tetrodes, between CA1 tetrodes, or between CA1 and CA3 tetrodes. "OR" functions were set for CA1 and CA3 tetrodes to send a stimulus upon the detection of ripple activity on any channel, inhibiting all recorded hippocampal SWRs across channels.

Stimulation at Reward

In this experimental setup, subjects were continuously stimulated in 200 ms intervals for the entire duration while at the reward sites on the maze. A recently modified MATLAB algorithm allowed for the accurate onset of stimulation using the animal's x-y coordinates that were recorded with the Neuralynx tracking system. Stimulation was automatically turned on as soon as subjects entered the area in the immediate vicinity of the reward location, and periodic stimulation stayed on until subjects left the area, as shown in Figure 4. Stimulation strength was determined prior to experimentation using I/O curves, as described above (Establishing Stimulation Perimeters). In each session, trials were separated into stimulation and no-

stimulation blocks, which were typically comprised of 3 or 4 trials. Sessions often ended with no-stimulation trials to confirm recovery of the network and to control for general effects of the stimulation in comparison to direct effect of eliminating SWR.

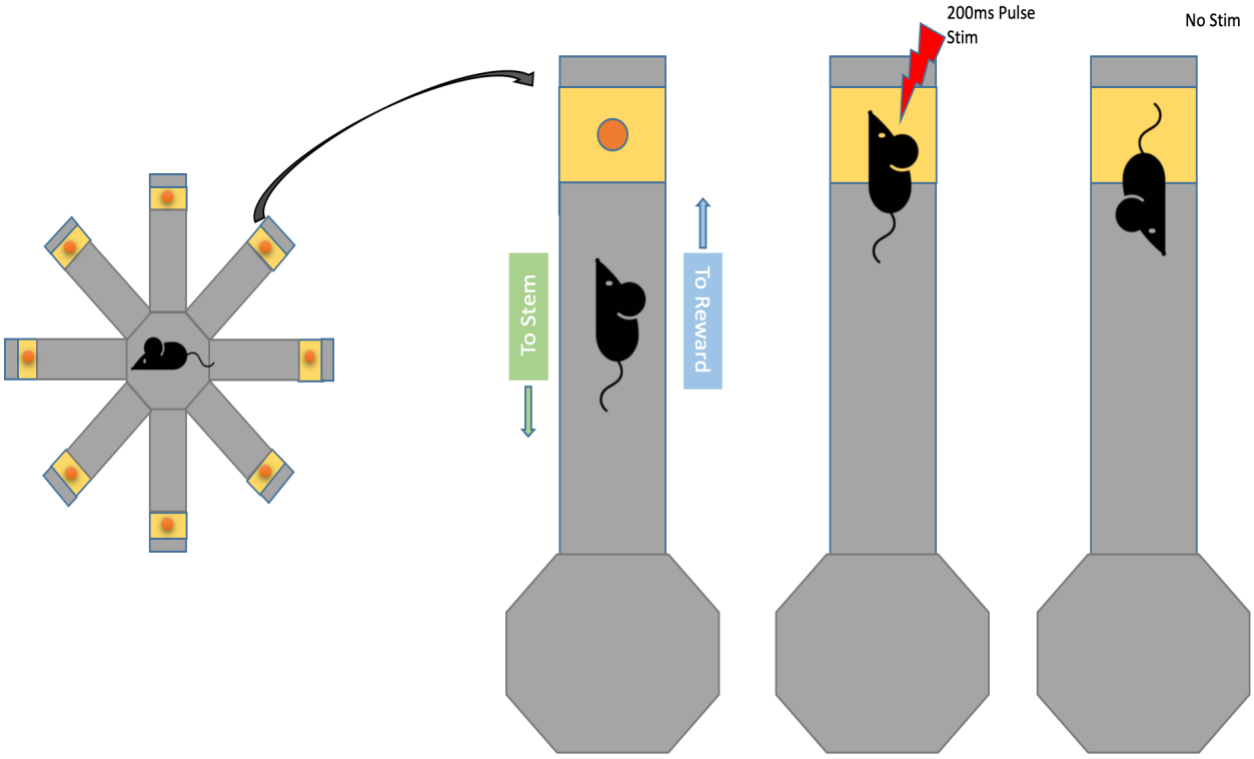

Figure 4. Stimulation at Reward Experimental Paradigm. Rodents were stimulated at reward location at the end of each arm on stimulation trials, and stimulation was turned off on control trials. Continuous stimulation in 200 ms intervals was automatically administered when the animal was positioned in the vicinity of the reward location and stopped as soon as the animal exited the reward site.

Histology

After completing the final recording session, implanted subjects were euthanized with administration of high dosage of pentobarbital. Immediately after, an intracardial perfusion procedure took place where subjects first received ~300 mL of phosphate buffered saline (PBS) followed by ~200 ml of 4 % paraformaldehyde (PFA) in PBS. Post-perfusion, subjects were set aside for at least 2 hours to ensure fixation of the brain around the tetrodes for better

reconstruction of tracks. Afterwards, tetrodes were raised and the brain was extracted to be placed in 4 % PFA for 24 hours. The brain was then transferred to a 30 % sucrose in PBS solution to be equilibrated which took approximately 2 days. After this period, the brain was frozen and 40 micrometer coronal sections were obtained using a microtome. Sections were then mounted onto micro-slides and left to dry for 48 hours. At this point, sections were stained with cresyl violet to label hippocampal cells and to detect end locations of tetrodes for verification of recording sites. High-resolution images of the right hippocampus in the anterior to posterior direction were taken using a microscope to visualize tetrode tracks and locations. Images of the vHC were also obtained to confirm the location of the two stimulation wires.

Tetrode Tracking

Utilizing the obtained images from histology, hippocampal sections with identifiable tetrode tracks were matched to the map of the implanted drive and specific tetrode locations. Positions of tetrodes were determined using directionality of the coronal slices (Anterior to Posterior) and were compared to the arrangement of the tetrode bundle. The deepest points of tetrodes were assigned as the final locations and were verified to be either in the CA1 or CA3 cell layers. The two stimulating wires were also similarly confirmed to be resting in the vHC.

Statistical Analysis

Data included in the study was tested for normality and presented as mean ± standard deviation with analysis done using Microsoft Excel. Performance data was averaged across animals, and two-sided t-tests were performed when appropriate. The null hypothesis was rejected when $P<0.05$.

CHAPTER II – RESULTS

Simultaneous recordings from the hippocampal CA1 and CA3 sub-regions

In order to address our central question, we first needed stable extracellular recordings from the hippocampus, more specifically the CA3 cell layer, to have access to LFP data. This was achieved with the use of a hyper-drive which allowed for the placement of 14 independently moveable tetrodes in different hippocampal cell layers. Through the use of independently moveable tetrodes, rather than a singular probe, we were able to record from different regions simultaneously. This was beneficial as it allowed for the recoding of LFP across DG, CA1, and CA3 cell layers. Previous studies have mainly focused on SWR events occurring in the CA1 region (Buzsaki, 2015). However, we looked to record primarily from the CA3 region while also simultaneously recording from the CA1 to allow for comparative analysis between SWRs generated from each layer. Therefore, in each animal, 10 of the 14 tetrodes were lowered down to the CA3 region with using the LFP profile as a guide. Two tetrodes were kept in the CA1 layer. Finally, two reference tetrodes were kept in the cortex and fissure, respectively. Placement of tetrodes was strategized to maximize the breadth of recordings from different regions and optimize unit detection. Later, histological imaging revealed that some tetrodes were positioned in the most lateral extent of the hippocampus resulting in the passing of the CA3 layer without encountering any cells. Also, throughout the course of lowering the tetrodes, a small number of tetrodes were presumed to be stuck due to the lack of change in the local field potential upon turning. This may have been the result of microglia forming around the tetrode and rendering it immovable, or a malfunction in the mechanics of the drive. Postmortem histology confirmed the location of most recording tetrodes in the CA3 cell layer (Figure 5). This verified that our recordings were from the appropriate regions of interest, validating our data and analysis.

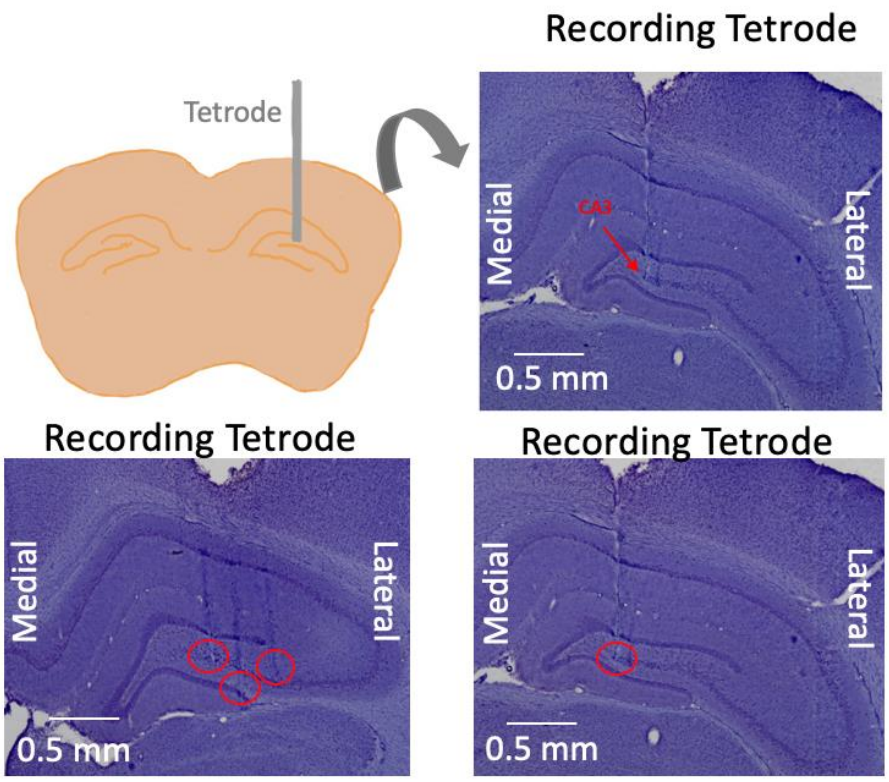

Figure 5. Hyper-drive Tetrode Tracking Analysis. Histological confirmation of the placement of recording tetrodes in the CA3 layer of the hippocampus as circled in red. Cresyl violet stained 40 μm slices from anterior to posterior ends of the brain enabled tracking of the final locations of all tetrodes.

Stimulation of the vHC and the subsequent inhibition of hippocampal cells

With stable in-vivo recordings available, SWR oscillations could be studied further. To achieve our goal of demonstrating a casual role of CA3 SWR oscillations in ongoing working memory, manipulation of CA3-generated SWRs was necessary. This was achieved with the implementation of a stimulation protocol that ultimately resulted in the disruption of SWRs. In this protocol, the hippocampal network was silenced through electrical stimulation of the vHC which lead to a subsequent period of inhibition in neuronal firing. This effect is confirmed through the generation of peristimulus-time histograms which display the period of inhibition of

a single cell upon stimulation at a given amplitude (Figure 6A). In these histograms, cell spike counts are represented on the y-axis with time in milliseconds on the x-axis. This analysis was essential in proving the role of SWRs in working memory as quantification of behavioral performance in only informative if network inhibition can be confirmed. Various stimulation strengths were tested by plotting an input/output curve with each stimulus strength and its respective level of inhibition. These curves were used to select the optimal strength to achieve ~100 ms of inhibition in cell firing. This standard length of inhibition is set according to literature which has shown 100 ms of inhibition in CA1 cells to result in sufficient silencing of SWR activity to impair the learning of a working memory task (Jadhav et al, 2012). Therefore, with similar levels of inhibition, we could address whether there is a comparable effect during ongoing working memory when CA3 SWRs are silenced.

In experiments conducted, inhibition periods between 50 ms and 100 ms were typically attained in CA3 cells at varying stimulus strengths across animals (Rat 1011, 70 ms at 100 pA; Rat 1064, 100 ms at 170 pA; Rat 1065, 50 ms at 180 pA; Rat 1068, 100 ms at 120 pA). These results were often coupled with at least 100 ms of inhibition in CA1 cells, which proved to be easier to achieve. The limitation to producing greater levels of inhibition in the CA3 network was the induction of unwanted seizures at higher stimulus strengths, which were seen to lower inhibition thresholds after the fact. Given our results, sufficient inhibition of CA3 cells was possible, even though they were not inhibited as reliably as CA1 cells. Confirmation of sufficient inhibition levels verified that adequate silencing of hippocampal cells to disrupt SWR-associated activity could be achieved.

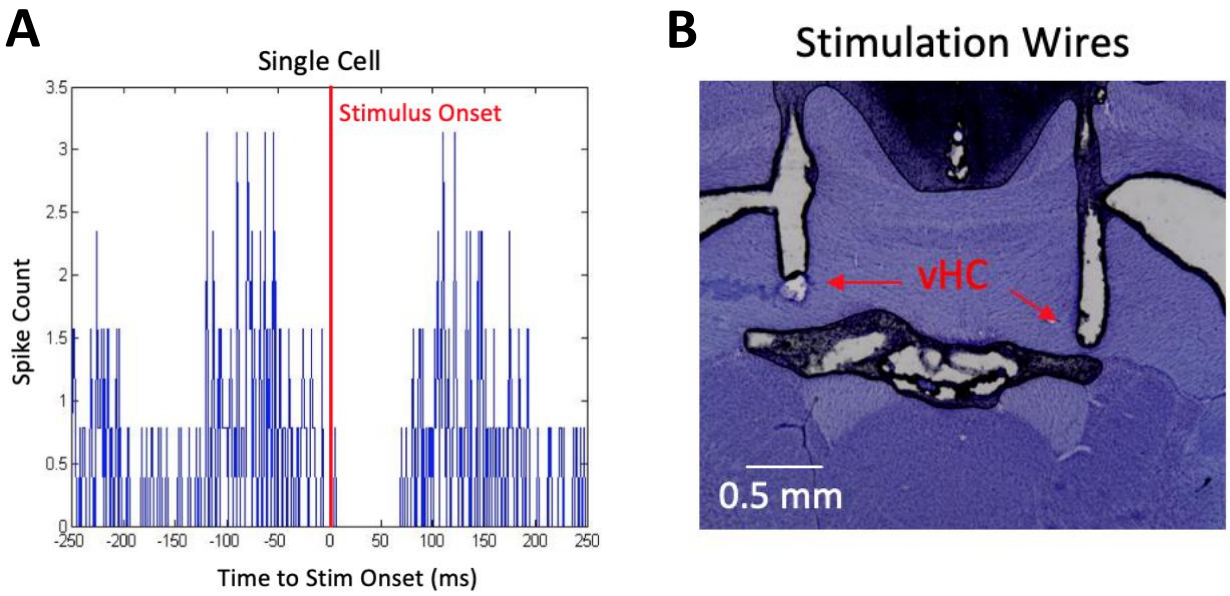

Figure 6. Inhibition Efficiency and Histological Confirmation of Stimulation Wires. (A) Peristimulus-time histogram showing inhibition of a CA3 cell upon stimulation. Time 0 represents the stimulus onset, and absence of spiking of the selected cell in the following ~50 ms confirms inhibition. (B) Verification of the bilateral placement of the stimulus wires in the vHC.

Accurate detection of SWR events required for the timely delivery of stimulus

In order to successfully truncate SWR events, we first needed to properly identify SWR events. Accordingly, an online detection algorithm was developed to accurately identify and label such events. SWRs possess identifiable features, such as high frequency oscillations, that allow for their classification as distinct events. The new closed-loop detection system implemented recognized high frequency population bursts in the LFP, shown in Figures 7A and B, and commanded stimulation of the vHC in response. As the standard method of detection, the Xilinx software processes an online detection program which calculates the LFP amplitude in a frequency band using an exponential moving average (EMA) method. In offline analysis, this method was compared to the standard method of using the root-mean-square of the ripple band (150 – 250 Hz) and of detecting a SWR when the root-mean-square exceeded 4 standard

deviations from its mean value. To set the most appropriate thresholds for accurate online detection of SWRs, threshold plots (Figure 7C) were generated. These plots present threshold values on the x-axis and the number of events detected by either the offline root-mean-square or the online EMS method at a given threshold on the y-axis. The threshold is selected by determining where the overlap between the number of SWR events detected with the online real-time method and with the offline method (which serves as the ground truth for number of SWR events) is maximal. This can be displayed as a Venn diagram where total number of SWRs detected by each method, as well as number of overlapping SWRs detected across the different methods is presented (Figure 7D). Greater overlap between the different methods signifies greater detection accuracy which can be confirmed for each recording tetrode present in the cell layer. The analysis can be repeated after the experiment is performed, and experiments with threshold values which produce unreliable SWR detection can be excluded from data analysis. This detection protocol has recently been developed and will be used in all experiments moving forward for determining the optimal detection threshold and the accuracy of the selected threshold. With the optimized detection of SWR events and sufficient inhibition of cells, SWR disruption experiments were warranted.

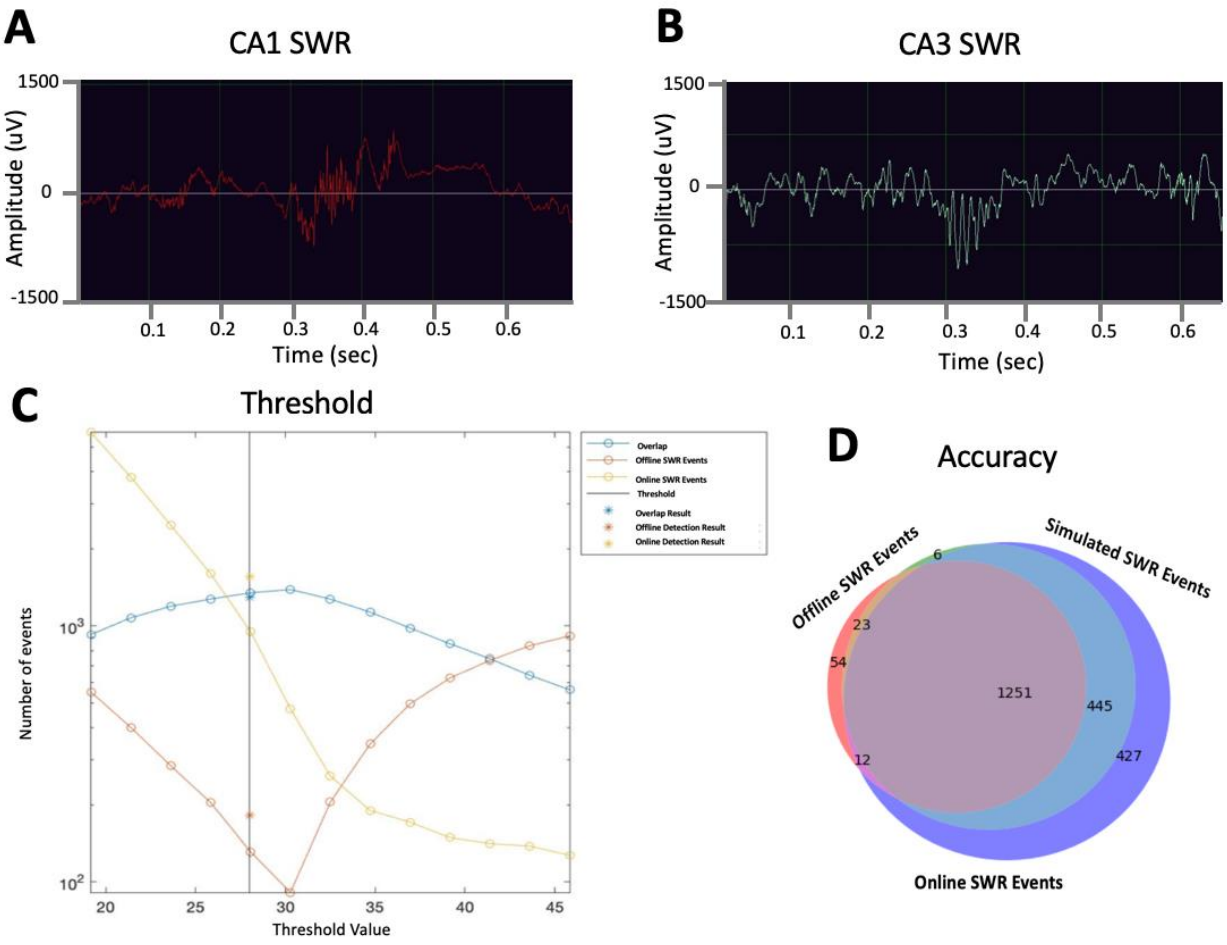

Figure 7. SWR Detection and Accuracy. (A) LFP trace of SWR event from the CA1 layer of the hippocampus. (B) LFP trace with SWR event from the CA3 layer of the hippocampus (C) Optimal threshold values for SWR detection were obtained by analyzing SWR detection with two different methods and by calculating the overlap (Detection with both methods, blue; detection with only offline method, red; detection with only online method, yellow). The offline detection was with a fixed threshold (4 SD) while the simulated online detection used the threshold plotted on the x-axis. The threshold that is actually used during the recording session is represented by the vertical line. (D) Online SWR detection (light and dark blue) in comparison to offline detection (orange) with the overlap in purple.

Preliminary data from SWR detection experiments suggested no behavioral effect upon disruption

Given the recent development of the detection system, data from 2 animals, 1064 and 1065, who underwent successful SWR inhibition experiments is presented. Two recording sessions with similar detection logics are analyzed for each animal. The mean percent performance for each animal on no-stimulation and stimulation trials is displayed (Figure 8A and B). The reported performance values are the calculated mean from two experimental days. In Figure 8A, rat 1064 performed two stimulation upon SWR detection experiments on two separate days. The logic implemented on both days was an "AND" function where the animal was stimulated every time there was SWR events on either both CA1 channels or both CA3 channels. Therefore, both CA1 and CA3 SWR events would be detected and a stimulus sent under this logic. Rat 1064 completed a total of 40 trials (24 no-stim trials and 16 stim trials) with a mean performance of 92.3% on no-stimulation trials and 95.5% on stimulation trials. Contrary to our expectations, there was a slight improvement in performance when SWRs were truncated.

In Figure 8B, the performance of rat 1065 across two days of stimulation on detected SWR events is reported. The logic implemented in these experiments was an "OR" function where stimulation was administered every time a SWR event was detected on any channel. Similar to an "AND" function, both CA1 and CA3 SWRs were disrupted under this logic, however, stimulation occurs much more frequently as coherence between channels is not a criterion for detection. Eighteen trials without stimulation and 18 trials with stimulation were completed across two days where rat 1065 performed with 92.8% accuracy on no-stimulation trials and 81.3% on stimulation trials. Here we see a clear deficit in this animal's performance when SWRs were inhibited. This contradicts the performance data from the previously presented animal where there was a slight improvement. In order to address this discrepancy in results,

more SWR inhibition experiments need to be performed across multiple animals to confirm the ultimate effect. The current variation in results may be due to chance, which can be tested in a larger data set. Also, the different outcomes may be due to the different logics used for each animal. If not all SWR events within CA3 and within CA1 are coherent, then a higher proportion of SWRs will be silenced using the "OR" logic compared to the "AND" logic. To address this possibility, coherence of SWR events across the layers must be assessed.

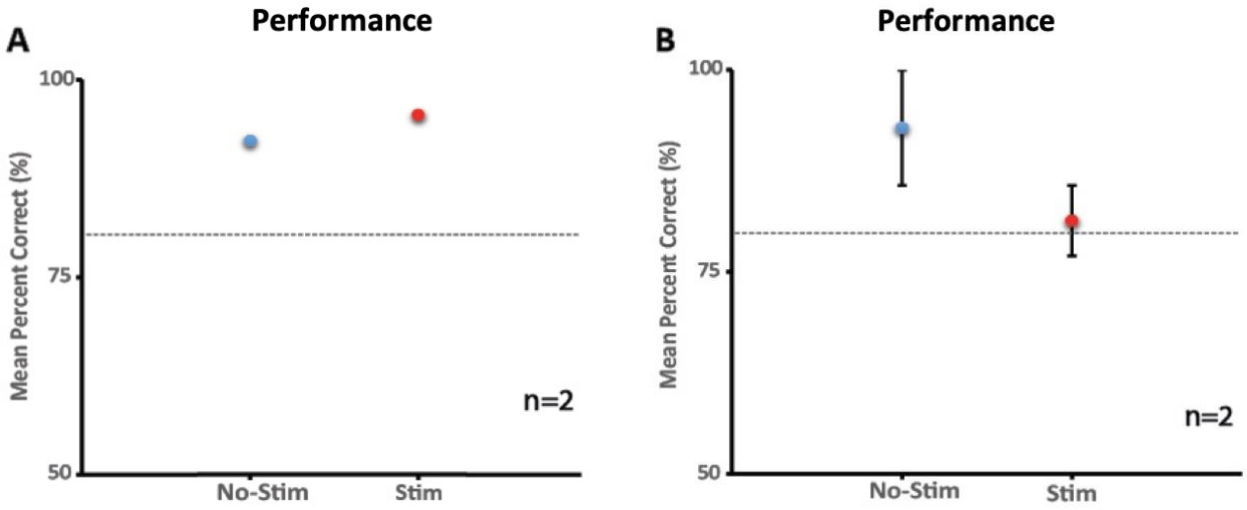

Figure 8. Performance of Rat 1064 and 1065 After SWR Disruption in the Working Memory Task. (A) Mean percent correct trials of rat 1064 from 2 sessions of stimulation upon SWR detection on a pair of CA1 and on a pair of CA3 tetrodes (B) Mean percent correct trials of rat 1065 from 2 sessions of stimulation upon SWR detection on any of four tetrodes (two in CA1 and two in CA3). Error bars indicate standard deviation.

Inhibition of hippocampal activity at the rewards sites on the maze revealed no significant impairment in performance

Considering there was no clear impairment when SWR events were truncated upon detection, a different type of hippocampal manipulation was performed for comparison. In these experiments, subjects received a train of stimuli at the reward sites on the maze, blocking not

only activity during SWRs, but also all other hippocampal activity while at the reward location. This approach was motivated by the finding that SWRs are most prominent at the reward sites during this exact task (Sasaki et al, 2018). Also, other interesting firing patterns were described at the reward site during this dentate-dependent task, including the preferential spiking of dentate granule cells (Sasaki et al, 2018). Therefore, this experiment was conducted to determine whether performance is independent of any CA3 neuronal activity occurring at reward locations. In these experiments, stimulation was administered by repeating stimulation pulses every 200 ms while the animal was positioned in the vicinity of any of the reward locations at the end of each arm. An online algorithm (implemented in MATLAB) was utilized in tandem with the tracking of x-y coordinates with the Neuralynx tracking system and stimulation was initiated upon the animal's entry into the defined region and ceased stimulation upon departure. Stimulation pulses thus continued throughout the entire duration of time the animal spent consuming rewards. The reported mean performances are from 4 different animals across 5 recording sessions N=5 (one animal performed 2 stimulation at reward experiments). The mean percent correct for trials without stimulation trials is 91.9 % with a standard deviation of 4.0 % (Figure 9A) and the mean percent correct for trials with stimulation 86.8 % with a standard deviation of 9.5 % (Figure 9A). Even though there seems to be a slight decrease in performance accuracy when stimulation is administered, a two-sided T-Test revealed there is no significant difference between the two value sets with a p-value of 0.3460.

Even though there seems to be no significant impairment in the animals' percent correct choices, observation of the rats' behavior during experiments raised the question whether animals change their strategy in performing the task when SWRs are inhibited and use other brain regions to complete the task instead. Therefore, we measured whether animals take more

time to complete stimulation trials compared to no stimulation trials. This can reveal any change in strategy as the animals would spend more time searching rather than knowing their exact next destination. Time stamps were noted at the beginning and end of each trial. The moment the first arm was raised marked the beginning of the trial and the moment the animal returned to the center stage marked the end. Analysis of the time data collected suggests there is no significant difference between the duration of stimulation trials and no-stimulation trials (p-value of 0.2118). The mean time to complete no-stimulation trials was 1.13 minutes with a standard deviation of 0.1 minutes while the mean time to complete stimulation trials was 1.24 minutes with a standard deviation of 0.2 minutes. Given these results, animals took approximately the same time to complete trials in which they were stimulated at the reward site and trials in which no stimulation took place (Figure 9B).

To further explore whether there was a change in strategy affecting the animals' behavior on the spatial working memory task when stimulation at the reward took place, a deeper analysis of the performance data was performed. Stimulation and no-stimulation trials during experiments were performed in sets of 3 or 4 trials. Stimulation and no stimulation sets were alternated in the duration of the task. Animals typically began and ended behavioral sessions with sets of no stimulation trials. The results show no significant difference between the first set of stimulation trials and last set of stimulation trials completed by the animals ($p<0.05$). Similarly, performances in the first set of no-stimulation and last set of no-stimulation trials showed no significant difference ($p<0.05$). This indicated there is no quantifiable change in the animal's performance and behavior in the presence or absence of disruption of hippocampal activity patterns in the vicinity of the reward locations. Because most SWRs occur at these locations, animals therefore seem to perform similarly on the task regardless of hippocampal activity that

would otherwise occur during these reward-related SWR events which were hypothesized to determine the animal's subsequent choice (Figure 9C).

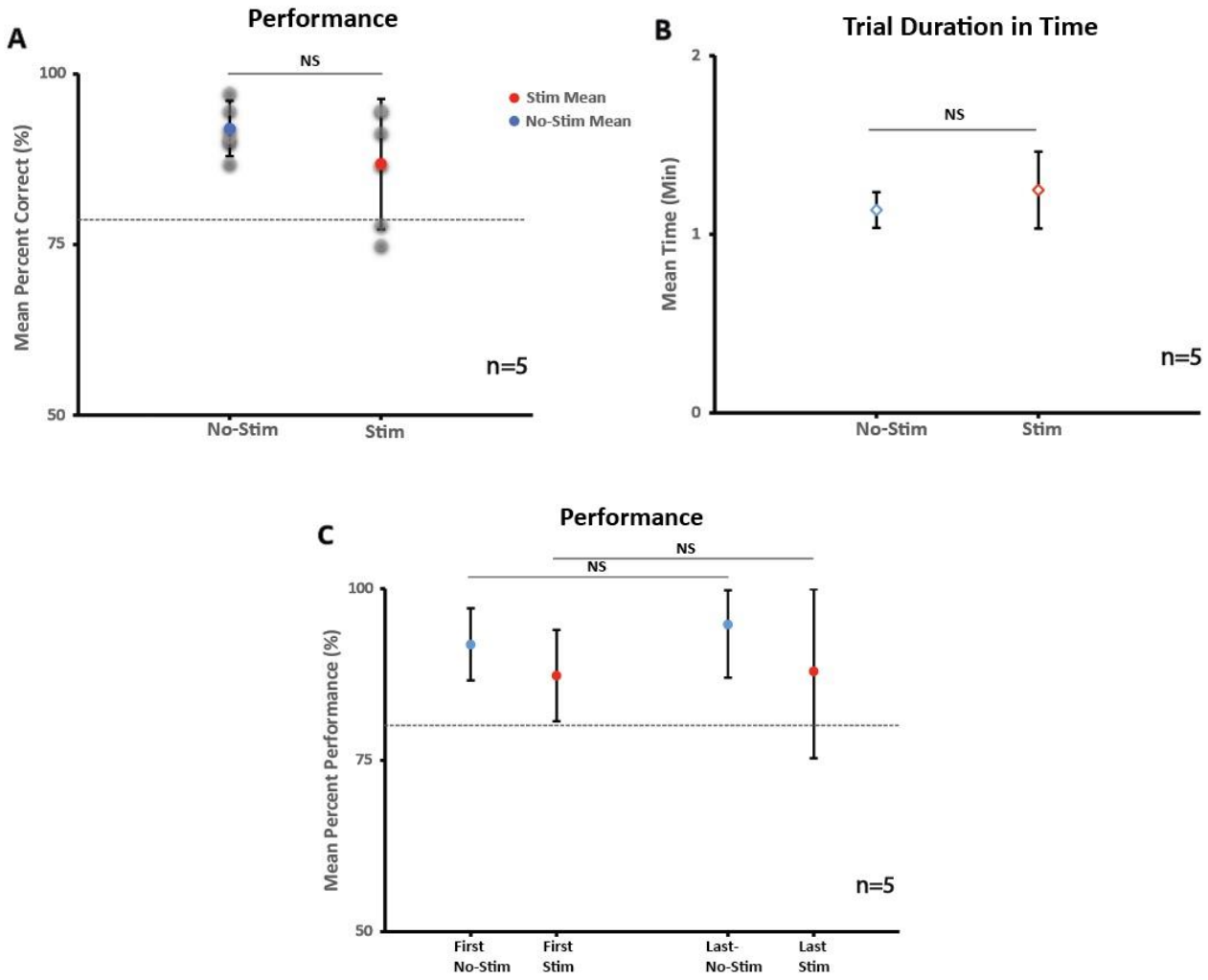

Figure 9. Inhibition of Hippocampal Neurons at the Reward Sites Did Not Result in a Significant Behavioral Impairment. (A) Mean percent performance from 5 recording sessions across 4 different animals (n=5) on stimulation and no-stimulation trials in stimulation at reward experiments. Gray dots represent the performance from the 5 recording sessions. The blue dot represents the mean across animals on no stimulation trials while the red dot represents the mean across animals on stimulation trials. There was no significant difference between trials where hippocampal activity is inhibited at the reward site and trials where hippocampal activity is unperturbed ($p<0.05$). (B) Mean time to complete no-stimulation and stimulation trials in stimulation at reward experiments. The blue rhombus indicates mean on no-stimulation trials while the red rhombus indicates mean on stimulation trials. There was no significant difference between time taken to complete trials in stimulation and no-stimulation trials ($p<0.05$). (C) Performance in sets (groups of 3 or 4 trials) of stimulation and no-stimulation trials as executed in experiments. Error bars indicate standard deviation.

Increase in vicarious searching behavior on trials with stimulation

Quantification of coarse behavioral measurements did not reveal a significant impairment in the number of correct choices during working memory tasks when SWRs are inhibited or when the hippocampus is inhibited at reward. However, we noted a change in searching behavior when stimulation is present during trials. Tracking the animal's position on the maze highlighted an interesting shift in the movement pattern of the animal while completing stimulated trials in comparison to control trials (Figure 10A-B). As illustrated in the figure, the animal's routes to the reward sites were very straight and direct in no-stimulation trials. However, when the animal was stimulated at the reward sites, its trajectories became indirect with more vicarious searching behavior. This finding suggests the animal became less certain about the next correct choice when hippocampal activity at the reward site was disrupted. This shift in the behavior was not detrimental to the choice accuracy as it did not result in a decrease in performance or an increase in duration of trials. Nonetheless, it is an interesting change in strategy that is worthy of further exploration, and it could suggest a change in the contribution of different brain regions in support of working memory processing.

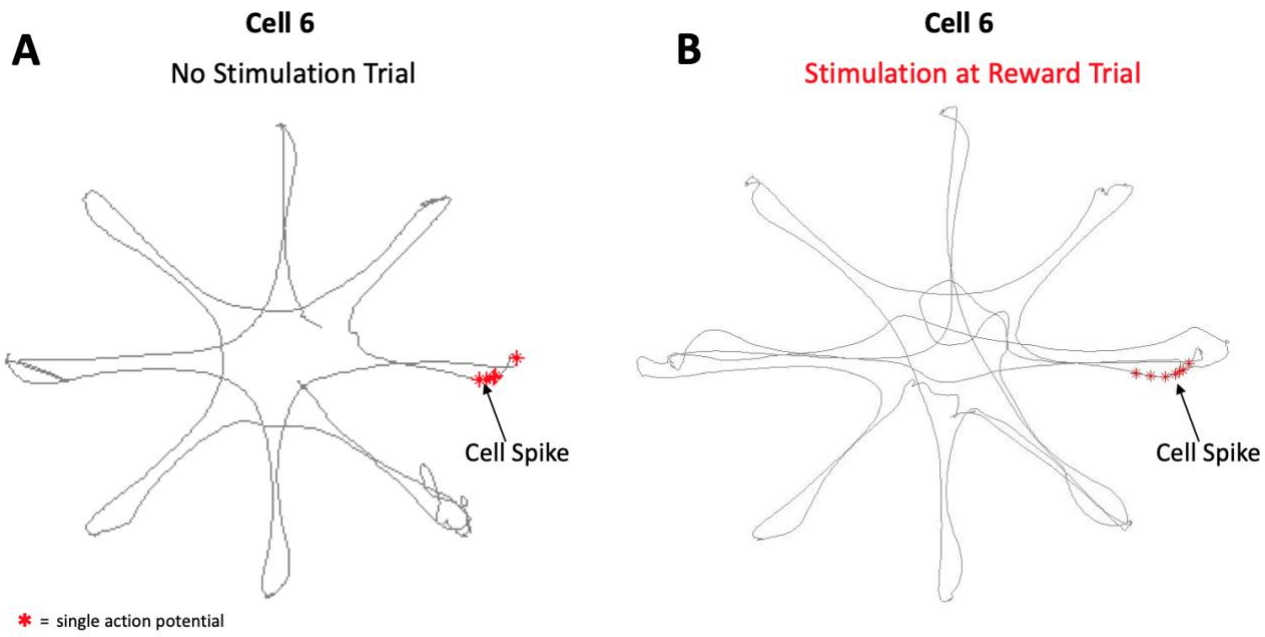

Figure 10. Positional Tracking of Animals on Stimulation and No-stimulation Trials. The behavior and strategy of animals in searching for rewards seemed to differ when brain stimulation was delivered at reward sites (A) Compared to when no stimulation was present (B). Tracked paths taken by the animal is shown as a grey line, spikes (i.e., single action potentials) of a hippocampal cell are shown as red dots.

CHAPTER III – DISCUSSION

SWR oscillations are high-frequency events detected in the CA1 and CA3 layers of the hippocampus during periods of immobility and slow-wave sleep (Frank and Joo, 2018). Research so far has led to speculations on the significance and contribution of these events in ongoing working memory. Many studies have explored the purpose and role of CA1 SWRs through local field potential and unit analysis and have demonstrated CA1 SWRs to be essential in the learning of working memory tasks as the speed of learning these tasks is impaired when SWR are silenced (Jadhav et al, 2012). This has been attributed to the disruption of place cells sequences that are replayed in both the forward and reverse directions during SWR events (Frank and Joo, 2018; Gupta et al, 2010). Even though many studies have addressed the content coded in these neuronal population bursts defined as ripples and their potential role in spatial working memory, their direct functionality in informing future decision making is yet to be demonstrated. Therefore, our project set out to further investigate CA3 SWR events and address their causal role in future decision making during dentate-dependent working memory tasks.

In our study, an 8-arm radial maze was utilized for the working memory task given that previous research has already established this task to be dentate dependent (Sasaki et al, 2018). This complex task also allows for statistically powerful analysis of behavioral performance which is critical in addressing our hypothesis. Previous studies have used linear or two-choice (T-maze or W-maze) tasks which were limited in error probability and in opportunities to analyze more complex behavioral sequences during ongoing working memory (Buzsaki, 2015; Gupta et al, 2010; Jadhav et al, 2012). On the 8-arm radial maze, probability of selecting correct choices due to chance is greatly reduced with the animal having 8 options to select from (Figure

1). This allows for a more precise assessment of working memory accuracy and dependence on SWR oscillations.

With a reliable working memory task established and rats trained to perform the task, stable LFP data was needed to meaningfully assess SWR events. This was achieved through the advancement of tetrodes to the hippocampal cell layers, and more specifically for our interests, the CA3 cell layer (Figure 5). In order to study the functionality of CA3 SWRs, we needed a method to truncate them and to quantify behavioral performance when these manipulations are performed. Disruption was accomplished through bipolar stimulating wires placed in the ventral hippocampal commissure (Figure 6B). This method was modeled similarly to previous studies where comparable measures were taken in inhibiting the generation of SWR events (Jadhav et al, 2012). Appropriate placement of stimulation wires enabled the administration of electrical stimuli at various strengths, resulting in the silencing of hippocampal cells and ultimately disrupting SWRs.

The most important aspect of demonstrating the causality of SWRs during behavior was the precise detection of these events. A significant breakthrough in our project was the development of a sophisticated SWR detection system which allowed for the accurate recognition of SWR events followed by timely stimulation and inhibition of activity. This was achieved with the optimization of already existing detection programs to appropriately identify the maximum number of genuine SWR events. The newly developed program is capable of simulating SWR detection during a full behavioral session given a short segment of data from which optimal threshold values for setting detection perimeters can be estimated (Figure 7D). Detection accuracy was checked post-experimentation, which confirmed reliability of our implemented method (Figure 7E).

Given the dentate-dependent working memory task, the means to appropriately record and detect SWR oscillations, and the stimulation measures in place, the stage was set for behavioral experiments. Subjects typically underwent two types of experiments while well-isolated cells were recorded. The first type of experiment implemented the novel SWR detection program to detect SWR events occurring during behavior and to truncate the events upon detection. Only 2 animals have performed such experiments so far given the recent development of the detection protocol. Therefore, the behavioral data available is not sufficient to make a firm conclusion. In one rat, the preliminary data suggests there is no impairment in the decision making of rodents in the working memory task when SWRs are inhibited compared to when they are not (Figure 8A). In a second rat, there seemed to be a slight decrease in performance accuracy (Figure 8B). This requires the collection of more data under similar experimental conditions to arrive at a definitive conclusion. Because the tool development process has now been completed, a streamlined method of data collection is available which may produce sufficient new data in the near future.

The second form of experimentation employed in our study is stimulation of subjects at reward sites to silence hippocampal activity altogether. This is a more general approach taken to serve as a control and confirm the reliability of the detection system. The logic for this experiment is in line with previous studies which demonstrated SWR events being most prominent at reward sites on the maze (Sasaki et al, 2018). Repeated stimulation of subjects during reward consumption disrupts all hippocampal activity taking place at that time, which includes SWR generation. Based on our results, disruption of the CA3 network at the reward sites on the maze does not lead to a significant impairment in the performance of rodents on working memory tasks (Figure 9A), although there was a trend towards an impairment. If the

results that there is no impairment holds up, it contradicts the popular belief held in the field that SWR oscillations play a role in the decision-making process of rodents during active working memory behavior (Foster and Pfeiffer, 2013). We did not only find that the performance remained accurate with and without SWR generation, but also found that animals also did not take any longer to complete trials with stimulation in comparison to trials without stimulation (Figure 9B). This further confirms the lack of impairment as an interrupted decision making process would postpone the completion of trials.

If SWRs are an essential factor in the working memory mechanism employed by rodents in complex spatial memory tasks, then their disruption should result in a significant impairment in behavior. As mentioned previously, SWR activity is correlated with inputs from the DG and the removal of the DG results in behavioral impairment (Sasaki et al, 2018). However, we show that SWR disruption on its own does not lead to a similar impairment in behavior. Our results, if confirmed, are inconsistent with the current understanding of the contribution of SWRs to memory processes and suggest that neuronal activity patterns during SWR oscillations are not necessary for working memory. Therefore, there may be other contributions from the DG to CA3, besides SWRs, that support ongoing working memory. For example, it is possible that firing patterns during theta states are more important for working memory than SWRs. If the collection of more data confirms our findings, these results will provide a new perspective on the function of SWR oscillations and spark more investigations on their underlying purpose.

CHAPTER IV – CONCLUSION

In summary, we were able to effectively manipulate hippocampal neuronal activity during CA3 SWR events and reward sites and did not find effects on performance of a working memory task. If confirmed, these results suggest that SWRs are not essential for the decision making process in completing such tasks. Moreover, the development of an optimized SWR detection protocol will facilitate efficient data collection from more subjects to be included in future studies. Our work will provide a better mechanistic understanding of the function of SWRs and on their causal role in supporting working memory processes.

REFERENCES

Anand, K., & Dhikav, V. (2012). Hippocampus in health and disease: An overview. In *Annals of Indian Academy of Neurology* Vol. 15, Issue 4, pp. 239-246 https://doi.org/10.4103/0972-2327.104323

Bakker, A., Kirwan, C. B., Miller, M., & Stark, C. E. (2008). Pattern separation in the human hippocampal CA3 and dentate gyrus. *Science (New York, N.Y.)*, *319*(5870), 1640–1642. https://doi.org/10.1126/science.1152882

Bragin, A., Jando, G., Nadasdy, Z., Hetke, J., Wise, K., & Buzsaki, G. (1995). Gamma (40-100 Hz) oscillation in the hippocampus of the behaving rat. *Journal of Neuroscience*, 15(1 I), 47–60. https://doi.org/10.1523/jneurosci.15-01-00047.1995

Buzsáki, G., Leung, L. W., & Vanderwolf, C. H. (1983). Cellular bases of hippocampal EEG in the behaving rat. *Brain research*, *287*(2), 139–171. https://doi.org/10.1016/0165 0173(83)90037-1

Buzsáki, György. (1986). Hippocampal sharp waves: Their origin and significance. *Brain Research*, 398(2), 242–252. https://doi.org/10.1016/0006-8993(86)91483-6

Buzsáki G. (2015). Hippocampal sharp wave-ripple: A cognitive biomarker for episodic memory and planning. *Hippocampus*, *25*(10), 1073–1188. https://doi.org/10.1002/hipo.22488

Colgin, L. L. (2016). Rhythms of the hippocampal network. In *Nature Reviews Neuroscience* Vol. 17, Issue 4, pp. 239–249. Nature Publishing Group. https://doi.org/10.1038/nrn.2016.21

Csicsvari, J., Jamieson, B., Wise, K. D., & Buzsáki, G. (2003). Mechanisms of gamma oscillations in the hippocampus of the behaving rat. *Neuron*, *37*(2), 311–322. https://doi.org/10.1016/s0896-6273(02)01169-8

Ebbinghaus H (1880) Urmanuskript "Ueber das Gedächtniß". Passau: Passavia Universitätsverlag.

Girardeau, G., Benchenane, K., Wiener, S. I., Buzsáki, G., & Zugaro, M. B. (2009). Selective suppression of hippocampal ripples impairs spatial memory. *Nature neuroscience*, *12*(10), 1222–1223. https://doi.org/10.1038/nn.2384

GREEN, J. D. (1964). The Hippocampus. In *Physiological reviews* Vol. 44, pp. 561 608. https://doi.org/10.1152/physrev.1964.44.4.561

Gupta, A. S., van der Meer, M. A., Touretzky, D. S., & Redish, A. D. (2010). Hippocampal replay is not a simple function of experience. *Neuron*, *65*(5), 695–705. https://doi.org/10.1016/j.neuron.2010.01.034

Jadhav, S. P., Kemere, C., German, P. W., & Frank, L. M. (2012). Awake hippocampal sharp wave ripples support spatial memory. *Science (New York, N.Y.), 336*(6087), 1454–1458. https://doi.org/10.1126/science.1217230

Joo, H. R., & Frank, L. M. (2018). The hippocampal sharp wave-ripple in memory retrieval for immediate use and consolidation. *Nature reviews. Neuroscience, 19*(12), 744–757. https://doi.org/10.1038/s41583-018-0077-1

JOUVET, M., & MICHEL, F. (1959). Corrélations électromyographique du sommeil chez le chat décortiqué et mésencéphalique chronique [Electromyographic correlations of sleep in the chronic decorticate & mesencephalic cat]. *Comptes rendus des seances de la Societe de biologie et de ses filiales*, *153*(3), 422–425.

Lashley, K. S. (1950). *In search of the engram.* In Society for Experimental Biology, *Physiological mechanisms in animal behavior. (Society's Symposium IV.)* (p. 454–482).

Leutgeb, S., Leutgeb, J. K., Barnes, C. A., Moser, E. I., McNaughton, B. L., & Moser, M. B. (2005). Independent codes for spatial and episodic memory in hippocampal neuronal ensembles. *Science (New York, N.Y.), 309*(5734), 619–623. https://doi.org/10.1126/science.1114037

Leutgeb, J. K., Leutgeb, S., Moser, M. B., & Moser, E. I. (2007). Pattern separation in the dentate gyrus and CA3 of the hippocampus. *Science (New York, N.Y.), 315*(5814), 961–966. https://doi.org/10.1126/science.1135801

Mankin, E. A., Diehl, G. W., Sparks, F. T., Leutgeb, S., & Leutgeb, J. K. (2015). Hippocampal CA2 activity patterns change over time to a larger extent than between spatial contexts. *Neuron, 85*(1), 190–201. https://doi.org/10.1016/j.neuron.2014.12.001

Morris, R. G., Garrud, P., Rawlins, J. N., & O'Keefe, J. (1982). Place navigation impaired in rats with hippocampal lesions. *Nature, 297*(5868), 681–683. https://doi.org/10.1038/297681a0

MÜLLER GE, PILZECKER A. Experimentelle Beiträge zur Lehre vom Gedächtniss. *Zeitschrift für Psychologie. Ergänzungsband.* 1900;1:1–300.

Nabavi, S., Fox, R., Proulx, C. D., Lin, J. Y., Tsien, R. Y., & Malinow, R. (2014). Engineering a memory with LTD and LTP. *Nature*, *511*(7509), 348–352. https://doi.org/10.1038/nature13294

Nakazawa, K., Quirk, M. C., Chitwood, R. A., Watanabe, M., Yeckel, M. F., Sun, L. D., Kato, A., Carr, C. A., Johnston, D., Wilson, M. A., & Tonegawa, S. (2002). Requirement for hippocampal CA3 NMDA receptors in associative memory recall. *Science (New York, N.Y.), 297*(5579), 211–218. https://doi.org/10.1126/science.1071795

O'Keefe, J., & Dostrovsky, J. (1971). The hippocampus as a spatial map. Preliminary evidence from unit activity in the freely-moving rat. *Brain research*, *34*(1), 171–175. https://doi.org/10.1016/0006-8993(71)90358-1

Penfield, W., & Milner, B. (1958). Memory Deficit Produced by Bilateral Lesions in the Hippocampal Zone. *Archives of Neurology And Psychiatry*, 79(5), 475-497. https://doi.org/10.1001/archneurpsyc.1958.02340050003001

Penfield W, Boldrey E. Somatic motor and sensory representation in the cerebral cortex of man as studied by electrical stimulation *Brain*. 60: 389-443.

Pfeiffer, B. E., & Foster, D. J. (2013). Hippocampal place-cell sequences depict future paths to remembered goals. *Nature*, *497*(7447), 74–79. https://doi.org/10.1038/nature12112

Reber, P. U., Schmied, B., Seiler, C. A., Baer, H. U., Patel, A. G., & Büchler, M. W. (1998). Missed diaphragmatic injuries and their long-term sequelae. *The Journal of trauma*, *44*(1), 183–188. https://doi.org/10.1097/00005373-199801000-00026

Sasaki, T., Piatti, V. C., Hwaun, E., Ahmadi, S., Lisman, J. E., Leutgeb, S., & Leutgeb, J. K. (2018). Dentate network activity is necessary for spatial working memory by supporting CA3 sharp-wave ripple generation and prospective firing of CA3 neurons. *Nature neuroscience*, *21*(2), 258–269. https://doi.org/10.1038/s41593-017-0061-5

SCOVILLE, W. B., & MILNER, B. (1957). Loss of recent memory after bilateral hippocampal lesions. *Journal of neurology, neurosurgery, and psychiatry*, *20*(1), 11–21. https://doi.org/10.1136/jnnp.20.1.11

Sullivan, D., Csicsvari, J., Mizuseki, K., Montgomery, S., Diba, K., & Buzsáki, G. (2011). Relationships between hippocampal sharp waves, ripples, and fast gamma oscillation: influence of dentate and entorhinal cortical activity. *The Journal of neuroscience : the official journal of the Society for Neuroscience*, *31*(23), 8605–8616. https://doi.org/10.1523/JNEUROSCI.0294-11.2011

Suzuki, S. S., & Smith, G. K. (1988). Spontaneous EEG spikes in the normal hippocampus. V. Effects of ether, urethane, pentobarbital, atropine, diazepam and bicuculline. *Electroencephalography and clinical neurophysiology*, *70*(1), 84–95. https://doi.org/10.1016/0013-4694(88)90198-8

Treves, A. & Rolls, E. T. (1991) What determines the capacity of autoassociative memories in the brain?, Network: Computation in Neural Systems, 2:4, 371 397, DOI: 10.1088/0954-898X_2_4_004

Vanderwolf C. H. (1969). Hippocampal electrical activity and voluntary movement in the rat. *Electroencephalography and clinical neurophysiology*, *26*(4), 407–418. https://doi.org/10.1016/0013-4694(69)90092-3

van Strien, N. M., Cappaert, N. L., & Witter, M. P. (2009). The anatomy of memory: an interactive overview of the parahippocampal-hippocampal network. *Nature reviews. Neuroscience*, *10*(4), 272–282. https://doi.org/10.1038/nrn2614

Wilson, M. A., & McNaughton, B. L. (1994). Reactivation of hippocampal ensemble memories during sleep. *Science (New York, N.Y.)*, *265*(5172), 676–679. https://doi.org/10.1126/science.8036517

Wittner, L., & Miles, R. (2007). Factors defining a pacemaker region for synchrony in the hippocampus. *The Journal of physiology*, *584*(Pt 3), 867–883. https://doi.org/10.1113/jphysiol.2007.138131

Wood, E. R., Dudchenko, P. A., Robitsek, R. J., & Eichenbaum, H. (2000). Hippocampal neurons encode information about different types of memory episodes occurring in the same location. *Neuron*, *27*(3), 623–633. https://doi.org/10.1016/s0896-6273(00)00071-4

Xavier, G. F., & Costa, V. C. (2009). Dentate gyrus and spatial behaviour. *Progress in neuro psychopharmacology & biological psychiatry*, *33*(5), 762–773. https://doi.org/10.1016/j.pnpbp.2009.03.036

Ylinen, A., Bragin, A., Nádasdy, Z., Jandó, G., Szabó, I., Sik, A., & Buzsáki, G. (1995). Sharp wave-associated high-frequency oscillation (200 Hz) in the intact hippocampus: network and intracellular mechanisms. *The Journal of neuroscience : the official journal of the Society for Neuroscience*, *15*(1 Pt 1), 30–46. https://doi.org/10.1523/JNEUROSCI.15-01 00030.1995